










Investigation into the Axial Compression Behavior of Steel-Reinforced Concrete Columns with Square Steel Tubes Considering Initial Conditions

Cong Peng^{1,2}, Deprizon Syamsunur^{1,3*}, Taha Mohammed Jassam¹, Yonghui Wang¹, Salihah Suroi¹,
Muhammad Noor Hisyam¹, L. Oksri-Nelfia⁴

¹ Department of Civil Engineering, Faculty of Engineering, Technology and Built Environment, UCSI University, Kuala Lumpur 56000, Malaysia

² Department of Architecture and Civil Engineering, Guangxi Vocational College of Water Resources and Electric Power, Nanning 530023, China

³ Postgraduate Studies, Universitas Bina Darma Palembang, Kota Palembang 30111, Indonesia

⁴ Department of Civil Engineering, Faculty of Civil Engineering and Planning, Universitas Trisakti, Jakarta 11440, Indonesia

Corresponding Author Email: deprizon@ucsiuniversity.edu.my

Copyright: ©2024 The authors. This article is published by IETA and is licensed under the CC BY 4.0 license (<http://creativecommons.org/licenses/by/4.0/>).

<https://doi.org/10.18280/mmep.110804>

ABSTRACT

Received: 8 May 2024

Revised: 18 July 2024

Accepted: 24 July 2024

Available online: 28 August 2024

Keywords:

initial stress, square steel tube filled with steel-reinforced concrete columns, steel-encased concrete composite column, axial compression behavior, numerical simulation

This research offers an in-depth exploration of the mechanical behavior of square steel tubular columns reinforced with concrete under axial compression. The study particularly focuses on how initial conditions, including initial stress and structural defects, influence the columns' performance. By employing ABAQUS for finite element analysis, the investigation covers a broad spectrum of slenderness ratios, systematically assessing how these factors affect the structural integrity of the columns. The analysis reveals that while initial stress tends to reduce the peak load-bearing capacity, it paradoxically enhances the ductility of the columns, a critical aspect of their performance under load. Conversely, initial defects, particularly in slender columns, exacerbate instability, leading to significant reductions in load-bearing capacity. These findings highlight the pivotal role of initial conditions in shaping the mechanical behavior and overall safety of steel-reinforced concrete columns. The study's insights contribute to a deeper understanding of the load-bearing mechanisms and provide a robust framework for improving the precision and dependability of structural design. By integrating considerations of initial conditions into the design process, engineers can significantly bolster the safety and durability of composite columns, especially in high-risk applications such as high-rise buildings and bridges.

1. INTRODUCTION

Steel-reinforced concrete-filled steel tubular columns, compared to traditional concrete-filled steel tubular (CFST) columns, provide benefits such as enhanced bearing capacity and improved seismic performance. Consequently, these columns are extensively utilized in high-rise structures and bridge construction [1]. In practical engineering, the steel tube initially serves as a vertical support, carrying part of the structural load. When concrete is added, it increases the bearing capacity but introduces initial stress in the steel tube before forming a composite structure with the concrete [2]. Additionally, during laying and hoisting, geometric deviations in the steel tube can cause initial stress deviations, leading to defects in the structure even before it bears any load [3]. These initial stresses and defects reduce the overall bearing capacity of the components and alter the load distribution within the structure. Understanding how initial conditions impact the load-bearing capacity of concrete-filled steel tubular columns is crucial for improving design, ensuring structural integrity, and enhancing safety in high-rise buildings and bridges.

Due to the complex stress state of SRCFST structures, research on the influence of initial conditions on the bearing mechanism of these components is relatively scarce. Recent investigations into the effects of initial stress and defects on the mechanical behavior of components primarily examine ordinary concrete-filled steel tubular columns. Research indicates that initial stress in these columns accelerates the elasto-plastic stage of the outer steel tube, postpones the interaction between the steel tube and core concrete, diminishes the confining stress of the steel tube on the concrete during early loading phases, and ultimately reduces the overall stiffness and load-bearing capacity of the component [4, 5]. The influence of initial stress and slenderness ratio on the component's stiffness and load-bearing capacity is substantial; greater initial stress and slenderness ratio lead to a more significant reduction in the ultimate bearing capacity of the column [6-10]. Through experimental and theoretical approaches, Yao and Han [11], and Li et al. [12] formulated empirical equations to calculate the bearing capacity of concrete-filled steel tubular columns considering initial stress.

For steel-reinforced concrete-filled steel tubular

components, the constraint mechanism of the concrete shifts once the steel section is embedded. The steel section and steel tube together provide constraint for the concrete within the steel section, while the concrete outside the steel section is constrained by the steel tube. If the outer steel tube experiences initial stress, the constraint mechanism for both the internal and external concrete is altered, thereby impacting the component's overall bearing performance. This is especially significant for square steel tubular concrete columns, where the outer steel tube's constraint is primarily concentrated at the corners. Initial stress makes the steel tube at the corners more susceptible to yielding or buckling during loading, reducing the constraint effect on the concrete at weaker sections. This condition is particularly crucial for square steel tubular concrete columns, given that the constraint of the outer steel tube is predominantly concentrated at the corners. When initial stress is applied, the steel tube at the corners is prone to yielding or buckling early in the loading process. This early deformation weakens the constraint effect on the concrete, particularly in the weaker sections, leading to a potential reduction in overall structural integrity. For square steel tubular concrete columns, initial stress can cause the steel tube at the corners to yield or buckle first, reducing the constraint on weaker concrete sections. However, it is difficult to obtain changes in the contact force between steel and concrete through experimental methods alone. Therefore, it is necessary to use finite element methods to further understand the interaction between the internal components of SRCFST columns, facilitating a more detailed analysis of changes in overall bearing capacity.

For studies considering initial defects, existing research methods mainly fall into two categories. The first is the consistent defect mode approach, where initial geometric imperfections are introduced to the component in a specific configuration to simulate their effect on the component's bearing performance [13-16]. The second is the random defect mode method, which considers the arrangement and size of the initial defects in the structure to be random and normally distributed [17-20]. However, for CFST structures, the impact of overall defects on bearing performance is more significant. Therefore, introducing the defect application method of buckling mode can accurately simulate the deviations in position and size during construction. SRCFST components are more susceptible to initial stress and defects during construction, such as during initial hoisting and loading. If the influence of the initial state is not explicitly considered during construction, it can result in an overestimation of the structure's overall load-bearing capacity. This is particularly concerning in regions with low seismic design levels, where the axial compression ratio of columns is generally high. Components weakened by initial stress and defects are more likely to fail under high loads. Therefore, examining the effects of initial stress and defects on the axial compression performance of square steel tubular, steel-reinforced concrete columns is essential.

This study employs the finite element software ABAQUS to model axial compression tests on square steel tubular concrete-filled steel-reinforced columns, accounting for initial stress and defects. By examining the influence of initial stress and defects on load-displacement curves, stress distribution across sections, and contact force magnitudes in specimens with various slenderness ratios, the research delves into the bearing mechanism of these columns under initial conditions. The results aim to inform the design of steel-reinforced

concrete components' bearing capacity in construction projects.

2. FINITE ELEMENT SIMULATION

2.1 Modeling method

2.1.1 Material constitutive

Using the numerical simulation software ABAQUS, this study examines the axial mechanical behavior of square steel tubular columns reinforced with concrete and steel, taking into account initial stress and defects. Models were established for ordinary columns, columns with initial defects, and columns with initial stress under axial load. Each model consists of four components: the steel tube, I-shaped steel reinforcement, concrete, and end plates. Since the compression model of square steel tubular steel-reinforced concrete columns with initial stress is similar to that of ordinary square steel tubular steel-reinforced concrete columns, ABAQUS's plastic damage model (CDP) is employed for modeling the core concrete. The CDP model distinguishes between the material's tensile and compressive behaviors, effectively describing the irreversible damage and stiffness degradation of concrete. For the compressive stress-strain relationship, Han's [21] constitutive model for concrete-filled square steel tubular columns is adopted. This model captures the essential characteristics and behavior of the concrete under compressive loading, ensuring accurate simulation results and reliable predictions of the columns' performance under axial loads. The expression for this model is as follows:

$$y = \begin{cases} 2x - x^2, & x \leq 1 \\ \frac{x}{\beta_0(x-1)^\eta + x}, & x > 1 \end{cases} \quad (1)$$

where, $x = \frac{\varepsilon}{\varepsilon_{c0}}$; $y = \frac{\sigma_c}{\sigma_{c0}}$; $\sigma_{c0} = f'_c$; $\xi = \frac{f_{ys}A_s}{(f_c A_c)}$; $\varepsilon_{cc} = \varepsilon_c + 800 \cdot \xi^{0.2} \cdot 10^{-6}$; $\eta = 1.6 + 1.5/x$; $\beta_0 = \frac{(f'_c)^{0.1}}{1.2\sqrt{1+\xi}}$.

The ABAQUS's isotropic elastoplastic model is employed for the constitutive behavior of the steel tube and section. The stress-strain relationship utilizes Han's secondary plastic flow constitutive model for low-carbon steel [21], which is expressed as follows:

$$\sigma_s = \begin{cases} E_s \varepsilon_s, & \varepsilon_s \leq \varepsilon_1 \\ -A\varepsilon_s^2 + B\varepsilon_s + C, & \varepsilon_1 \leq \varepsilon_s \leq \varepsilon_y \\ f_y, & \varepsilon_y \leq \varepsilon_s \leq \varepsilon_2 \\ f_y \left[1 + 0.6 \frac{\varepsilon_s - \varepsilon_2}{\varepsilon_3 - \varepsilon_2} \right], & \varepsilon_2 \leq \varepsilon_s \leq \varepsilon_3 \\ 1.6f_y, & \varepsilon_s \geq \varepsilon_3 \end{cases} \quad (2)$$

where, $\varepsilon_1 = 0.8f_y/E_s$; $\varepsilon_y = 1.5\varepsilon_1$; $\varepsilon_2 = 10\varepsilon_y$; $\varepsilon_3 = 100\varepsilon_y$; $A = 0.2f_y/(\varepsilon_y - \varepsilon_1)^2$; $B = 2A\varepsilon_y$; $C = 0.8f_y + A\varepsilon_1^2 - B\varepsilon_1$.

2.1.2 Selection of elements and definition of contacts

To effectively analyze the influence of initial stress in the steel tube on the mechanical performance of square steel tubular steel-reinforced concrete columns, and given the regular shape of the finite element model and ease of mesh generation, 8-node reduced integration 3D solid elements (C3D8R) are utilized for all component instances. This approach enhances computational efficiency, reduces model

stiffness, and facilitates result convergence.

The interaction between the steel tube and concrete is modeled using normal and tangential surface-to-surface contact. Tangential behavior follows the Coulomb friction model with a friction coefficient of 0.5, while normal behavior is set to hard contact to prevent mesh penetration. The I-shaped steel section is embedded into the concrete matrix using the Embed method. The end plate's interaction with other components is defined by the Tie constraint, ensuring a rigid connection.

2.1.3 Meshing and boundary conditions

The model analysis is conducted in two stages. Initially, initial stress and defects are applied to the component. To apply initial stress to the steel tube, the initial stress coefficient β_s is determined, and then the initial stress is applied as a load to the steel tube in the finite element model. By editing the keyword "initial conditions, type=stress" in the ABAQUS input file, the initial stress field of the steel tube obtained from the simulation is imported into the axial compression model. This enables the finite element simulation of the axial compression bearing capacity of the concrete-filled steel tube with initial stress.

Initial defects are introduced using the consistent defect mode method, where the first-order buckling mode is incorporated into the model before applying the axial load. The boundary conditions are defined with one end fixed and the other end constrained in all directions except the loading direction, where the degree of freedom is released to apply the displacement load. The model's schematic diagram is shown in Figure 1.

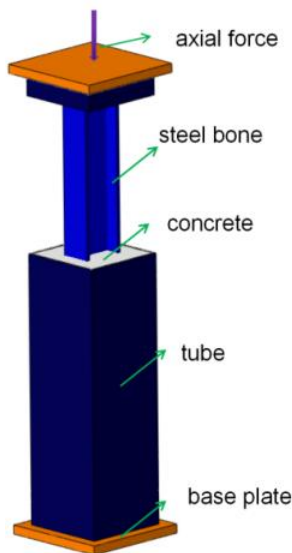


Figure 1. Finite element model

To ensure computational efficiency and mesh convergence, all elements are meshed using the structured meshing technique available in ABAQUS. Trial calculations indicate that when the element size is less than $H/30$ (with H representing the specimen's height), the element size minimally affects the finite element model results. Therefore, for computational efficiency, this study uses an element size of 20 mm. During meshing, efforts are made to align the element seeds between contacting elements, which improves computational accuracy and efficiency and helps avoid convergence issues.

2.2 Model verification

To validate the finite element model's accuracy, typical specimens from the literature [22, 23] were selected for comparison. This validation included analyzing the failure modes and load-displacement curves of these specimens. Figures 2 and 3 show the failure modes of two specimens with lengths $L=600$ mm and $L=2400$ mm under axial compression loads. For the short column under axial compression, both the experimental and finite element simulation specimens exhibit a bulging-type strength failure characteristic. For the long column, both show a bending-type instability failure mode.

Figure 4 presents a comparison between the load-displacement curves obtained from both experiments and simulations. The simulated curves match well with the experimental curves in overall trend peak values, and other aspects, with errors within 10%. Figure 4(c) demonstrates the mesh convergence validation, where the pseudo strain energy (ALLAE) is less than 1% of the internal energy (ALLIE), indicating good mesh convergence. Therefore, the numerical model established in this study is effective and can be used for subsequent data analysis.

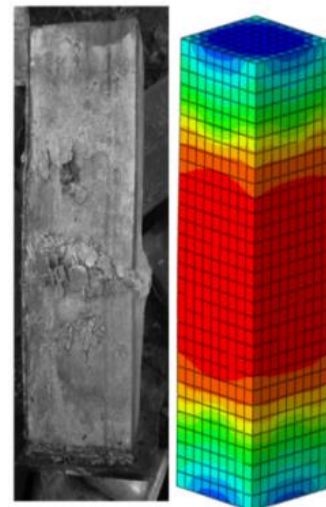


Figure 2. Axial compression failure

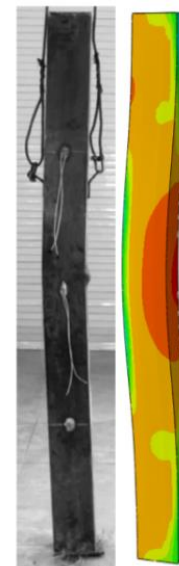


Figure 3. Buckling failure

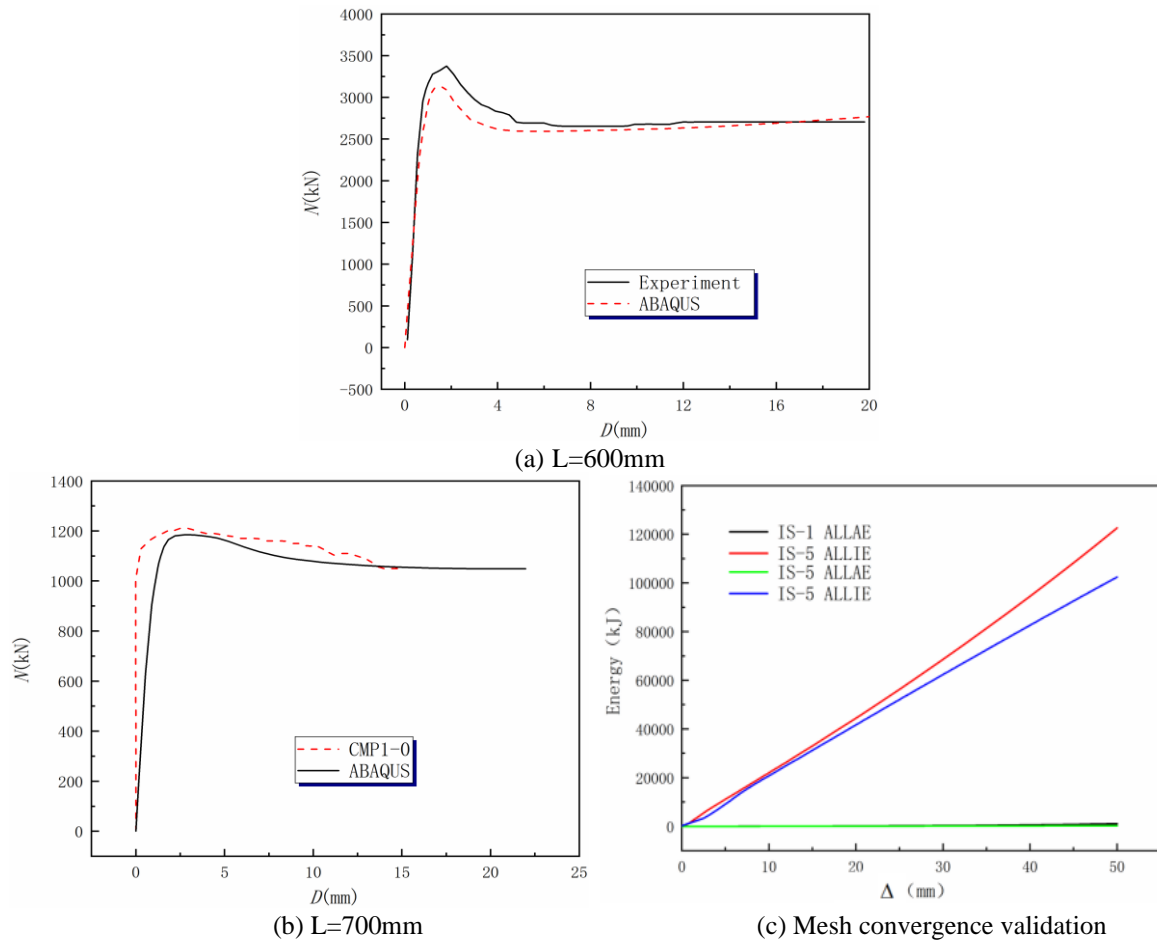


Figure 4. Model data validation

3. ANALYSIS OF STRUCTURAL BEHAVIOR UNDER INITIAL STRESSES AND INITIAL DEFECTS

3.1 Model parameter selection

Utilizing the validated numerical model previously described, a model of a square concrete-filled steel tubular (CFST) short column with embedded L-shaped steel was developed. This model aims to analyze the mechanical behavior of these components under conditions of initial stress and defects. Table 1 provides the primary parameters of the specimens. The specimens have a side length $b=195$ mm, steel

tube wall thickness $t=4.5$ mm, and total length $L=600-2500$ mm. The steel tube has a yield strength of 289 MPa, while the steel section has a yield strength of 338 MPa. The concrete is designed with a target strength of C60. The I-section steel used is 132b, with sectional dimensions of $100 \times 70 \times 5 \times 7$ mm and a steel ratio of 3.9%. Initial defects are introduced with a magnitude of $L/1000$ to simulate the positional and dimensional deviations occurring during construction. The technical specification for CFST structures [24] states that the initial load applied during construction must not exceed 40% of the steel tube's bearing capacity. Consequently, in this study, the initial stress coefficient is set to 0.34.

Table 1. Key parameters of specimens

No.	L (mm)	B (mm)	T (mm)	i	Fc (MPa)	Fs (MPa)	Fa (MPa)	β_s	N (KN)
N-1	600	195	4.5	10.7	48.1	289	338	0.34	3134
II-1	600	195	4.5	10.7	48.1	289	338	0	3106
IS-1	600	195	4.5	10.7	48.1	289	338	0.34	2711
N-2	1000	195	4.5	17.8	48.1	289	338	0.34	3109
II-2	1000	195	4.5	17.8	48.1	289	338	0	3108
IS-2	1000	195	4.5	17.8	48.1	289	338	0.34	2704
N-3	1500	195	4.5	26.6	48.1	289	338	0.34	2970
II-3	1500	195	4.5	26.6	48.1	289	338	0	2938
IS-3	1500	195	4.5	26.6	48.1	289	338	0.34	2662
N-4	2000	195	4.5	35.5	48.1	289	338	0.34	2863
II-4	2000	195	4.5	35.5	48.1	289	338	0	2789
IS-4	2000	195	4.5	35.5	48.1	289	338	0.34	2614
N-5	2500	195	4.5	44.4	48.1	289	338	0.34	2707
II-5	2500	195	4.5	44.4	48.1	289	338	0	2580
IS-5	2500	195	4.5	44.4	48.1	289	338	0.34	2532

Notes: 'N' refers to specimens subjected to normal loading; 'II' denotes specimens with initial defects under loading; 'IS' signifies specimens loaded with initial stress.

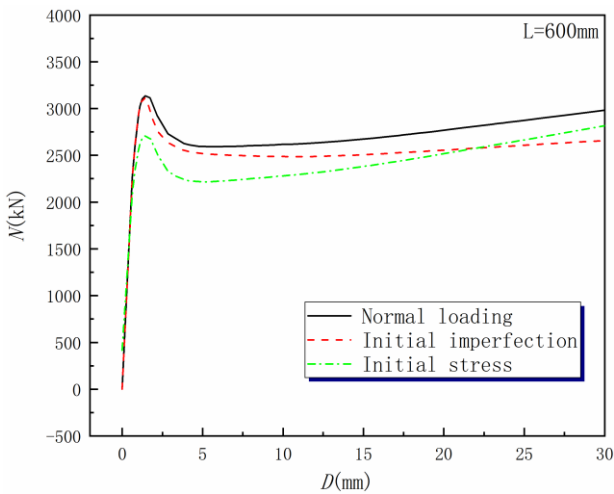
The initial stress coefficients calculated as follows:

$$\beta_s = \frac{\sigma_s}{\phi_s \cdot f_y} \quad (3)$$

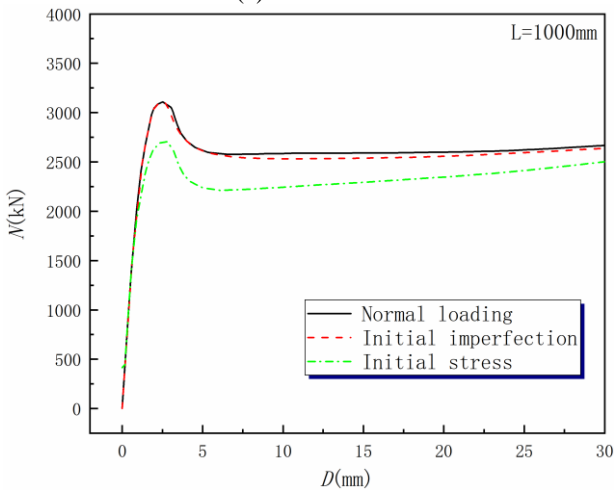
here, σ_s represents the initial stress of the steel tube, ϕ_s denotes the axial compression stability coefficient for the steel tube element, and f_y signifies the yield strength of the steel material.

3.2 Load-displacement curve

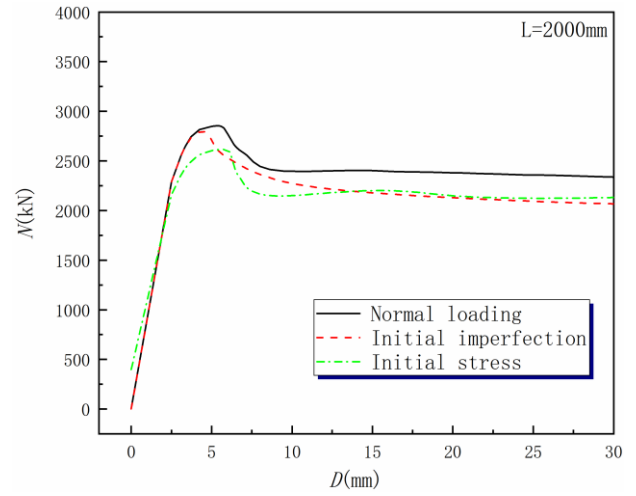
Figure 5 illustrates the load-displacement curves of the specimens, clearly showing that the loading process can be divided into four distinct stages: elastic, elasto-plastic, bearing capacity decline, and bearing capacity stabilization, each representing a specific phase in the mechanical behavior of the material. For axially compressed short columns (slenderness ratio $i < 20$), the peak load of the specimens does not change significantly after applying initial defects. However, for medium and long columns (slenderness ratio $i > 20$), the peak bearing capacity of the specimens decreases after introducing initial defects, and this reduction progressively increases. The reduction rates for columns II-3, II-4, and II-5 are 1.1%, 2.6%, and 4.7%, respectively. Introducing initial defects also accelerates the downward trend in the latter part of the load-displacement curve, leading to a reduction in the specimens' ductility. This change highlights the significant impact of initial defects on the structural integrity and performance of the columns.



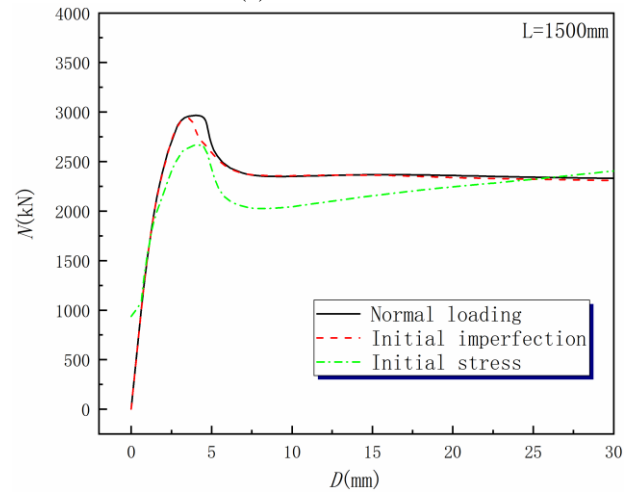
(a) L=600mm



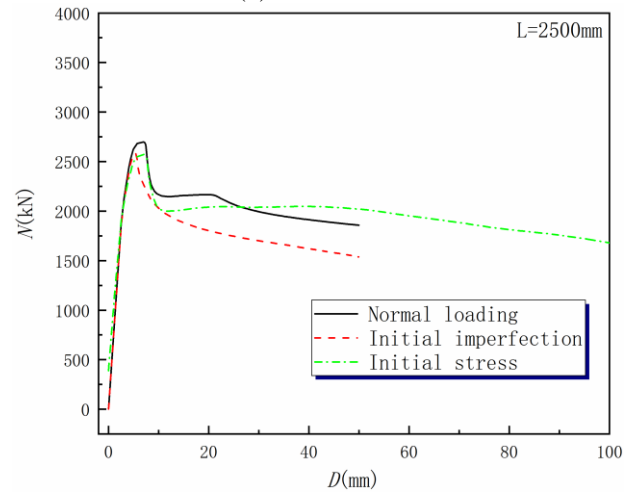
(b) L=1000mm



(c) L=1500mm



(d) L=2000mm



(e) L=2500mm

Figure 5. Load-displacement curves

When initial stress is applied, a significant decrease in the peak load of the specimens is observed; however, this reduction gradually lessens as the slenderness ratio increases. The peak bearing capacity reduction rates for columns IS-1 to IS-5 are 13.4%, 13%, 10.4%, 8.7%, and 6.5%, respectively. Meanwhile, applying initial stress improves the ductility performance of the specimens. It is evident that initial defects primarily influence the bearing performance of medium and long columns (slenderness ratio > 20). In contrast, the effect of initial stress on the bearing performance of the specimens diminishes as the slenderness ratio increases.

In reference to the displacement curves after the peak load, as illustrated in Figure 5(a), concrete axially compressed short columns primarily undergo strength failure when subjected to axial load. Consequently, once the curve attains the peak load, the steel tube's constraint effect on the concrete is heightened. This enhancement causes the softening phase of the concrete to progress slowly, allowing it to retain a high strength. The steel tube itself reaches the strengthening stage, increasing in strength. Additionally, due to compression expansion, the bearing cross-section increases. Therefore, without considering the uneven failure of the concrete during the test, the bearing capacity after the peak load would tend to increase.

As shown in Figure 5(e), before the instability failure occurs in concrete axially compressed long columns, the strength after the peak load slightly increases, similar to concrete short columns. Introducing initial stress causes the steel tube to attain a higher constraint stress earlier, resulting in a significantly higher strength after the peak load compared to when no initial stress is present. However, after the instability failure occurs, the load-displacement curve decreases.

3.3 Section load distribution

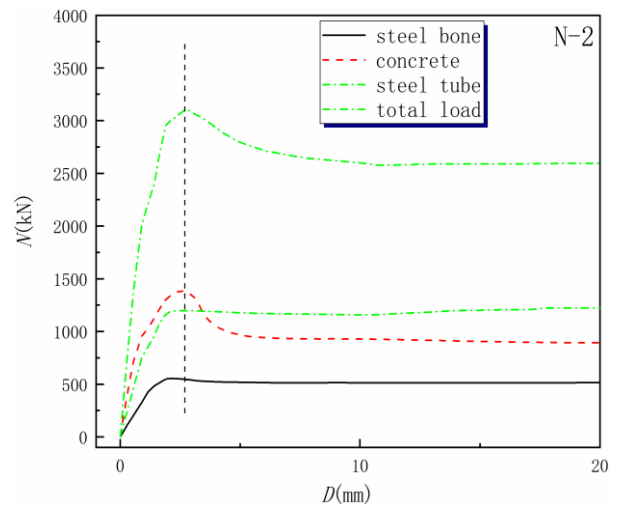
The collaborative work of each component in the square steel tubular steel-reinforced concrete column specimens is a major factor in their bearing capacity. The load-displacement curves for short columns ($L=1000$ mm) and long columns ($L=2000$ mm) at the mid-section (1/2 section) are extracted and compared, as illustrated in Figure 6 and Figure 7. The resulting data is summarized in Table 2. The bearing capacity of the specimens is primarily supported by the concrete, steel tube, and steel section before the peak load is reached. Once the peak load is exceeded, the concrete undergoes strain softening, reducing the specimens' overall bearing capacity.

Figure 6(a) shows that for specimens with a low slenderness ratio, the bearing capacity change in components with initial defects is minimal. For specimens experiencing initial stress, the components are already bearing the load at zero relative displacement during the loading phase, attributed to the initial stress in the steel tube. At this stage, the steel tube has not exerted normal confinement on the concrete and has already yielded. Further loading causes local buckling, reducing confinement stress on the concrete and decreasing the overall bearing capacity.

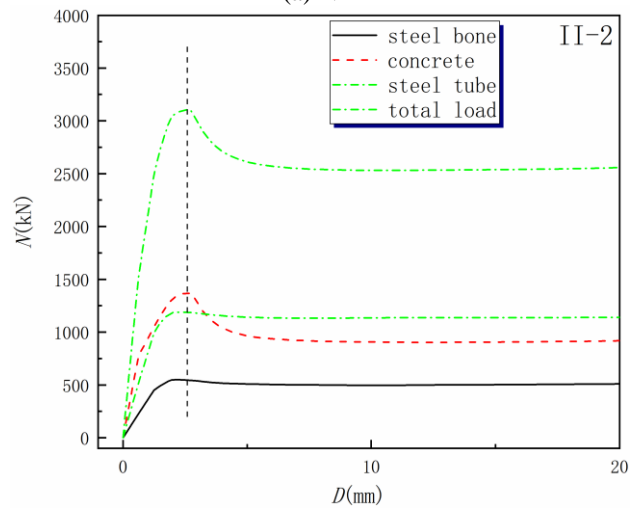
Figure 6(b) demonstrates that when the slenderness ratio of specimens is large, the model calculation results indicate that these specimens mainly experience instability failure. Introducing initial defects lowers the peak loads compared to ordinarily loaded specimens, indicating more severe bending instability. As slenderness increases, instability failure precedes strength failure. In these cases, although initial stress causes early yielding of the steel tube, local buckling does not occur before bending failure, thus reducing the impact of initial stress on peak bearing capacity.

Table 2. Model calculation data

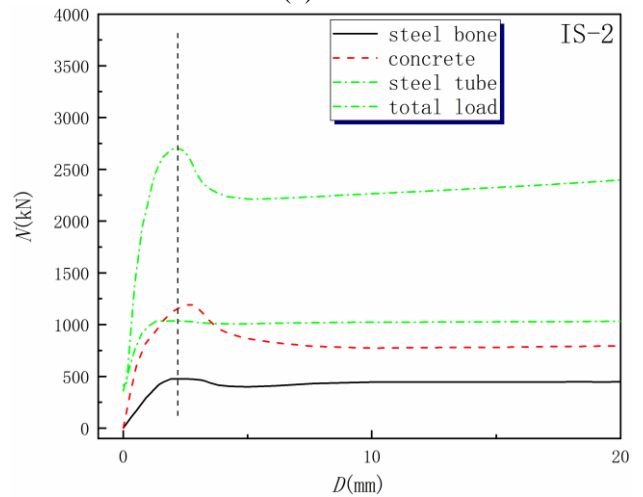
No.	Component Bearing Capacity (KN)				Contact Pressure (MPa)
	Steel Tube	Concrete	Steel Bone	Total	
N-2	1392	1198	544	3134	14.5
II-2	1368	1186	552	3106	13.1
IS-2	1150	1035	526	2711	10.5
N-5	1189	1033	485	2707	7.7
II-5	1107	998	475	2580	7.5
IS-5	1098	978	456	2532	7.2



(a) N-2



(b) II-2



(c) IS-2

Figure 6. Load-deformation curves of individual components ($L=1000$ mm)

3.4 Analysis of contact pressure

The analysis of the contact pressure distribution in square steel tubular steel-reinforced concrete columns is depicted in Figure 8. The data indicates that the highest contact pressures are found at the corners of the concrete, suggesting that these regions are where the steel tube exerts the most significant constraint on the concrete. By examining the contact pressure at point A, situated at the mid-section (1/2 section) of the

specimens, it becomes evident that the lateral deformation of concrete is more pronounced in short columns during strength failure, in contrast to long columns during instability failure. This leads to higher contact compressive stress of the concrete on the steel tube in short columns, as shown in Figure 9, where the contact pressure for short columns ($L=1000$ mm) surpasses that of medium and long columns ($L=2500$ mm).

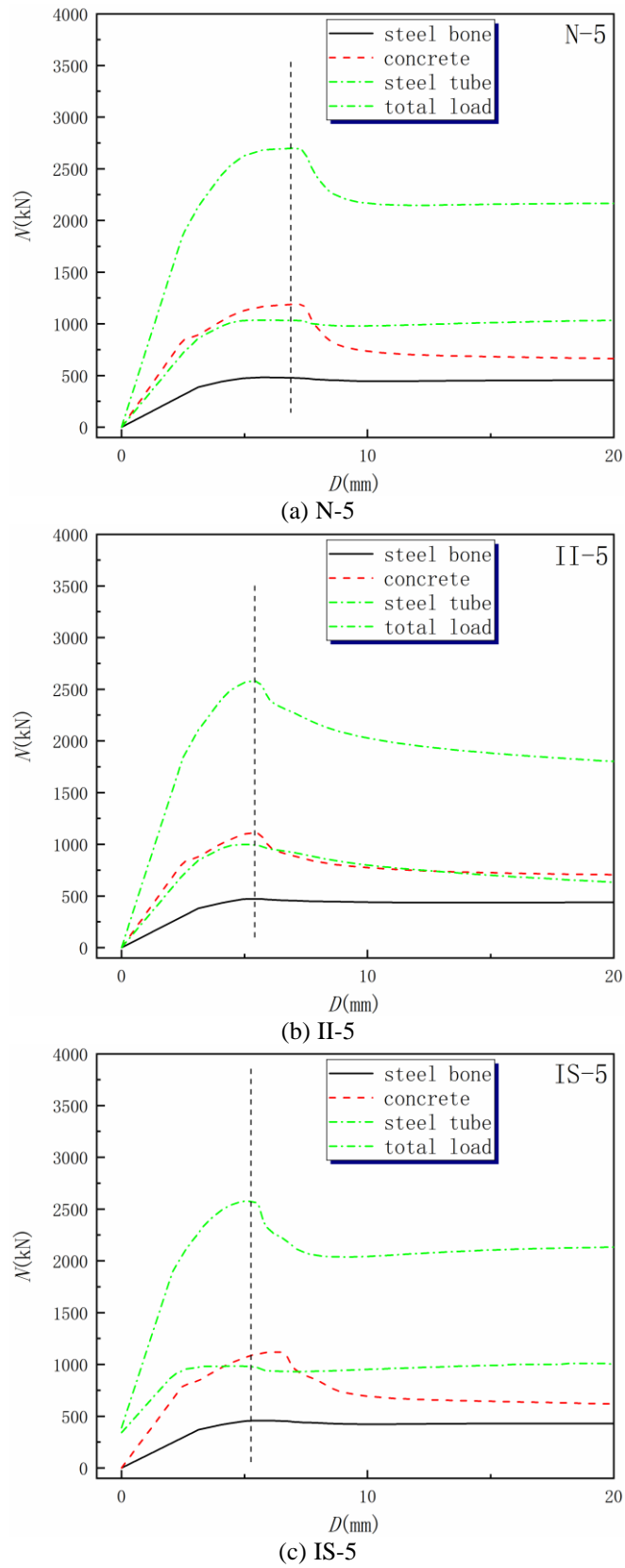


Figure 7. Load-deformation curves of individual components ($L=2500$ mm)

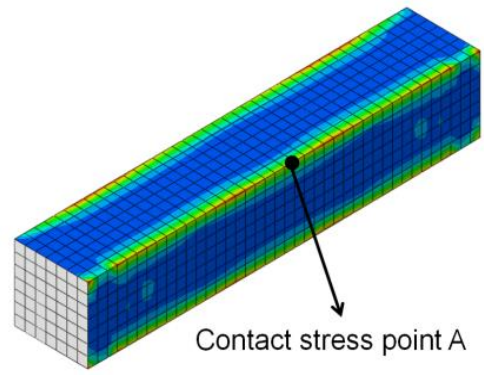


Figure 8. Contact pressure contour of concrete

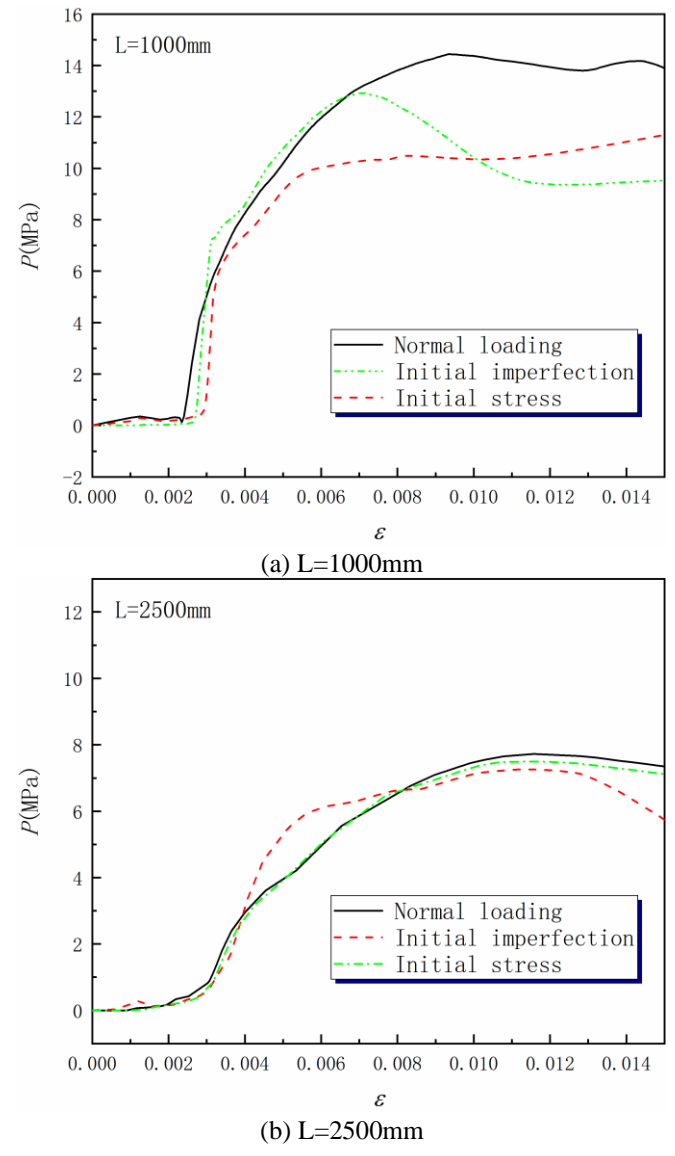


Figure 9. Contact pressure curve

Initially, during the loading process, the Poisson's ratio of the steel tube is greater than that of the concrete, resulting in less lateral deformation of the concrete relative to the steel tube, and thus no contact pressure is observed between them. As plastic deformation advances, the Poisson's ratio of the concrete progressively increases and eventually surpasses that of the steel tube. This progression leads the concrete to start exerting compressive pressure on the steel tube, enhancing the load-bearing capacity due to the confinement effect provided

by the steel tube.

For short columns ($L=1000\text{mm}$), the contact pressure is highest during normal loading. However, the influence of initial stress causes the steel tube to buckle upon entering the plastic stage, which reduces its contact pressure with the concrete. For long columns ($L=2500\text{ mm}$), the effect of initial stress is diminished by instability failure. This leads to no substantial alteration in the contact pressure between the concrete and the steel tube.

3.5 Concrete stress analysis

Figure 10 displays the longitudinal stress contour (S33) of the concrete at the final loading stage, showing that the failure mode of the specimens changes significantly as the slenderness ratio increases. The failure of short columns is primarily due to axial compression, whereas medium and long columns mainly experience instability failure. The longitudinal ultimate stress of the concrete in normally loaded specimens is higher compared to specimens with initial states.

The strong confinement provided by the steel framework near the steel section significantly increases the peak strength

of the concrete. This results in an 8-shaped constrained region in the stress contour adjacent to the steel section. For specimens with a length ($L=600\text{mm}$), initial defects have almost no impact on the longitudinal stress of the concrete. However, for specimens with initial stress, Due to the weak confinement effect of buckling, the maximum longitudinal stress in concrete decreased from 88 MPa to 77 MPa compared to the case without initial stress.

For specimens with a length ($L=2500\text{mm}$), the longitudinal stress distribution across the section is uneven during instability and failure. This uneven stress distribution is particularly pronounced in specimens with initial defects, as illustrated in Figure 10. Under the same loading displacement, the minimum longitudinal stress of the specimen containing initial defects is 1.79 MPa, indicating tensile stress. It can be concluded that specimens with initial defects experience more severe bending deformation compared to those without initial defects. The presence of initial stresses places the steel tube at a higher stress level, providing higher restraint stress to the concrete. Therefore, during the bearing phase after peak load, the ductility performance of the specimen is better with initial stress compared to without initial stress.

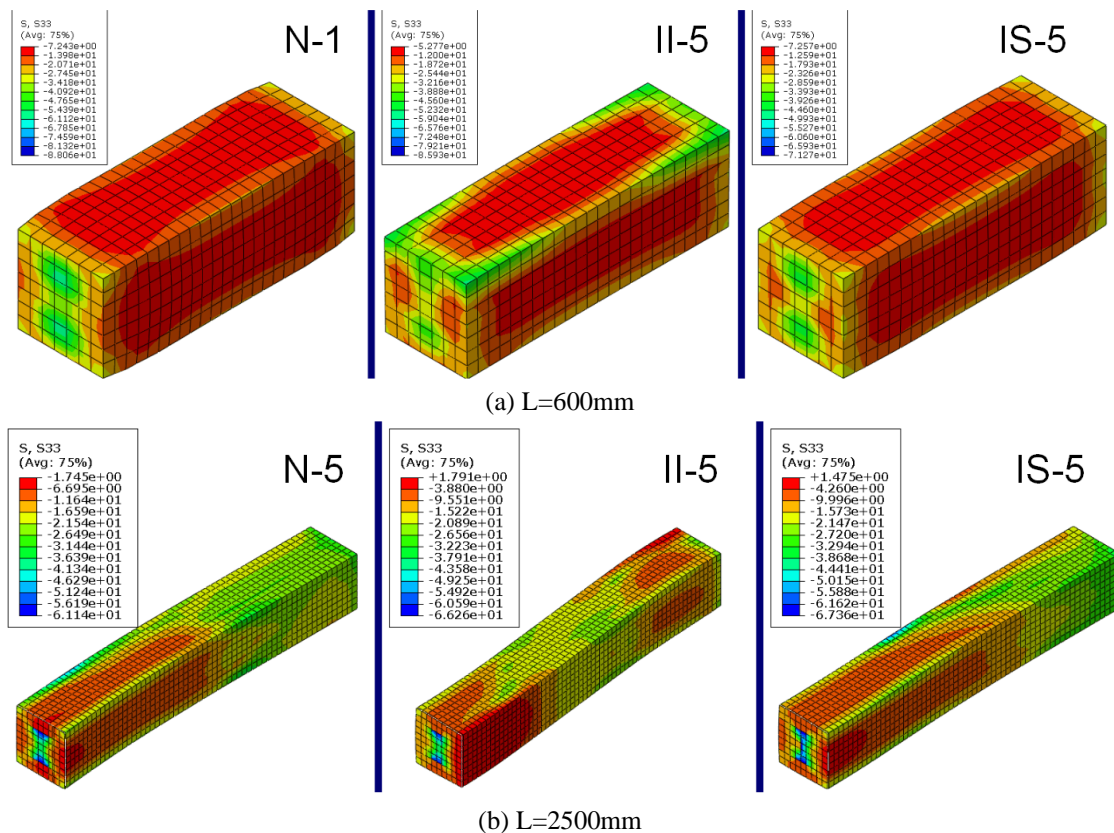


Figure 10. Longitudinal stress contour of concrete

4. CONCLUSIONS

The calculation process is divided into two stages by introducing initial defects in the specimens and initial stress in the steel tubes. The first stage involves calculating the effects of initial stress, followed by assessing the impact of initial defects. then importing the results as the initial state for the subsequent loading stage. This approach provides a finite element modeling method that considers the initial stress and initial defects from the construction process.

Compared to normal loading, the specimens' peak bearing capacity decreases after the application of initial defects and stress. As the slenderness ratio increases, the influence of initial stress on overall bearing performance gradually diminishes. For specimens with a length of 2500 mm, the reduction in overall bearing capacity due to initial stress decreases from 13.4% to 6.5%. Conversely, as the slenderness ratio increases, the impact of initial defects on the overall bearing performance gradually intensifies. For specimens with a length of 2500 mm, the reduction in overall bearing capacity

due to initial defects increases from 1.1% to 4.7%.

The introduction of initial stress causes the steel tube to yield and locally buckle earlier during the bearing process. At the buckling section, the steel tube's confinement effect on the concrete is weaker, reducing the concrete's compressive strength. Consequently, specimens with initial stress exhibit a lower peak bearing capacity compared to those without initial stress. However, the presence of initial stress enhances the steel tube's confinement stress on the concrete, resulting in better ductility during the post-peak load-bearing stage. Specimens with initial defects are more prone to instability failure due to the deformation caused by the buckling mode before loading.

In structural construction design, when the slenderness ratio (i) of a member is less than 20, introducing an initial stress coefficient ($\beta_s=0.34$) leads to a decrease in peak load of the specimen by more than 10%. Therefore, it is advisable to appropriately install external supports on the pipe to reduce the influence of initial stress on the structural bearing performance. When the slenderness ratio (i) of a member is greater than 20, a 1% reduction in the buckling mode decreases the peak load of the specimen by up to 4.7%. Therefore, during construction, it is crucial to minimize geometric deviations of the member to eliminate the impact of initial defects on the structure's bearing performance.

FUNDING

The paper was funded by the Basic Competence Improvement Project for Middle and Young Teachers in the Universities and Colleges of Guangxi (Grant No.: 2022KY1102).

REFERENCES

- [1] Ding, F.X., Zhang, T., Liu, X.M., Lu, Z.H., Guo, Q., Jiang, G.S. (2017). Behavior of steel-reinforced concrete-filled square steel tubular stub columns under axial loading. *Thin-Walled Structures*, 119: 737-748. <https://doi.org/10.1016/j.tws.2017.07.021>
- [2] Li, Y., Li, G., Hou, C., Zhang, W.J. (2019). Long-term experimental behavior of concrete-encased CFST with preload on the inner CFST. *Journal of Constructional Steel Research*, 155: 355-369. <https://doi.org/10.1016/j.jcsr.2019.01.001>
- [3] Zhang, R.L., Han, Z.F., Ma, L.N., Ning, G.X., Li, Z.Y., Gao, F. (2022). Influence of defect rate and location of core concrete on the bearing capacity of concrete steel tubular. *Building Structure*, 51(2): 78-84. <https://doi.org/10.19701/j.jzjg.2021.02.013>
- [4] Huang, F.Y., Chen, B.C. (2006). Experimental research on influence of initial stress to behavior of concrete filled steel tubular dumbbell shaped stub columns under axial loads. *Journal of Fuzhou University (Natural Science)*, 34(2): 240-244. <https://doi.org/10.3969/j.issn.1000-2243.2006.02.021>
- [5] Huang, F.Y., Chen, B.C., Lin, Y.Q., Sun, J.C. (2011). Research on hooping effect of concrete filled steel tube stubs with initial stress under axial compression. *Journal of Fuzhou University (Natural Science)*, 39(4): 575-580. <http://doi.org/10.7631/issn.1000-2243.2011.04.0575>
- [6] Huang, F., Yu, X., Chen, B., Li, J. (2016). Study on preloading reduction of ultimate load of circular concrete-filled steel tubular columns. *Thin-Walled Structures*, 98: 454-464. <https://doi.org/10.1016/j.tws.2015.10.015>
- [7] Liew, J.R., Xiong, D.X. (2009). Effect of preload on the axial capacity of concrete-filled composite columns. *Journal of Constructional Steel Research*, 65(3): 709-722. <https://doi.org/10.1016/j.jcsr.2008.03.023>
- [8] Han, L.H., Yao, G.H. (2003). Behaviour of concrete-filled hollow structural steel (HSS) columns with preload on the steel tubes. *Journal of Constructional Steel Research*, 59(12): 1455-1475. [https://doi.org/10.1016/S0143-974X\(03\)00102-0](https://doi.org/10.1016/S0143-974X(03)00102-0)
- [9] Xiong, D.X., Zha, X.X. (2007). A numerical investigation on the behaviour of concrete-filled steel tubular columns under initial stresses. *Journal of Constructional Steel Research*, 63(5): 599-611. <https://doi.org/10.1016/j.jcsr.2006.07.002>
- [10] Patel, V.I., Liang, Q.Q., Hadi, M.N. (2014). Behavior of biaxially-loaded rectangular concrete-filled steel tubular slender beam-columns with preload effects. *Thin-Walled Structures*, 79: 166-177. <https://doi.org/10.1016/j.tws.2014.02.013>
- [11] Yao, G.H., Han, L.H. (2004). Effects of initial stress of steel tubes on axial compression rigidity and flexural rigidity of concrete-filled steel tubular members. *Industrial Construction*, 7: 57-60. <https://doi.org/10.1007/BF02911033>
- [12] Li, W., Han, L.H., Zhao, X.L. (2012). Axial strength of concrete-filled double skin steel tubular (CFDST) columns with preload on steel tubes. *Thin-Walled Structures*, 56: 9-20. <https://doi.org/10.1016/j.tws.2012.03.004>
- [13] Zhang, B.W. (2018). Study on ultimate bearing capacity of CFST arch bridge considering initial stress and initial defect (MA Thesis). Harbin Institute of Technology. <https://kns.cnki.net/KCMS/detail/detail.aspx?dbname=CMFD201901&filename=1018894551.nh>
- [14] Li, Z.X. (2002). Effects of initial geometric defects on static and dynamic stability performance and bearing capacity of grid shell structures. *China Civil Engineering Journal*, 35(1): 11-15. <https://doi.org/10.1007/s11769-002-0073-1>
- [15] Wang, Z.B., Tao, Z., Han, L.H. (2006). Effect of initial imperfection on mechanical property of stub columns of square concrete-filled thin-walled steel tubes. *Industrial Construction*, (11): 19-22. [https://doi.org/10.1016/S1001-8042\(06\)60020-1](https://doi.org/10.1016/S1001-8042(06)60020-1)
- [16] Lyu, L., Zhang, X., Zhu, H., Guo, Z., Lu, S. (2018). Experimental study on bending performance of square concrete-filled steel tubular members with initial defects. *Journal of Wuhan University of Technology (Transportation Science and Engineering)*, 42(4): 705-709. <https://doi.org/10.3963/j.issn.2095-3844.2018.04.035>
- [17] Most, T., Bucher, C., Schorling, Y. (2004). Dynamic stability analysis of non-linear structures with geometrical imperfections under random loading. *Journal of Sound and Vibration*, 276(1-2): 381-400. <https://doi.org/10.1016/j.jsv.2003.07.038>
- [18] Schorling, Y., Bucher, C. (1998). Dynamic stability analysis for structures with geometrical imperfections. *Structural Safety and Reliability*, 2: 771-777.
- [19] Schorling, Y., Bucher, C. (1999). Stochastic stability of

- structures with random imperfections. *Stochastic Structural Dynamics*, 27: 343-348. https://www.researchgate.net/publication/240264824_Stochastic_stability_of_structures_with_random_imperfections.
- [20] Bielewicz, E., Gers, J. (2002). Shells with random geometric imperfections simulation- based approach. *International Journal of Non-Linear Mechanics*, 37(4-5): 777-784. [https://doi.org/10.1016/S0020-7462\(01\)00098-1](https://doi.org/10.1016/S0020-7462(01)00098-1)
- [21] Han, L.H. (2009). *Modern Composite Structures and Hybrid Structures*. Science Press.
- [22] Zhu, M., Liu, J., Wang, Q., Feng, X. (2010). Experimental research on square steel tubular columns filled with steel-reinforced self-consolidating high-strength concrete under axial load. *Engineering Structures*, 32(8): 2278-2286. <https://doi.org/10.1016/j.engstruct.2010.04.002>
- [23] Jia, Z.L., Shi, J.L., Wang, W.D., Xian, W. (2021). Study on compressive performance of steel-reinforced concrete-filled circular steel tubular members considering preload on steel tubes. *Journal of Building Structures*, 43(6): 63-74. <https://doi.org/10.14006/j.jzjgxb.2020.0796>
- [24] Technical Specification for Concrete-Filled Steel. (2014). *Tubular Structures*. China Architecture & Building Press.